journal

J. Am. Ceram. Soc., 79 [6] 1521–29 (1996)

# High-Temperature Tensile Behavior of a Boron Nitride-Coated Silicon Carbide-Fiber Glass-Ceramic Composite

Ellen Y. Sun*,*

Division of Engineering, Brown University, Providence, Rhode Island 02912

Steven R. Nutt*

Department of Materials Science, University of Southern California, Los Angeles, California 90089-0241

John J. Brennan*

United Technologies Research Center, East Hartford, Connecticut 06108

**Tensile properties of a cross-ply glass-ceramic composite were investigated by conducting fracture, creep, and fatigue experiments at both room temperature and high temperatures in air. The composite consisted of a barium magnesium aluminosilicate (BMAS) glass-ceramic matrix reinforced with SiC fibers with a SiC/BN coating. The material exhibited retention of most tensile properties up to 1200°C. Monotonic tensile fracture tests produced ultimate strengths of 230–300 MPa with failure strains of ~1%, and no degradation in ultimate strength was observed at 1100° and 1200°C. In creep experiments at 1100°C, nominal steady-state creep rates in the $10^{-9}$ $s^{-1}$ range were established after a period of transient creep. Tensile stress rupture experiments at 1100° and 1200°C lasted longer than one year at stress levels above the corresponding proportional limit stresses for those temperatures. Tensile fatigue experiments were conducted in which the maximum applied stress was slightly greater than the proportional limit stress of the matrix, and, in these experiments, the composite survived $10^5$ cycles without fracture at temperatures up to 1200°C. Microscopic damage mechanisms were investigated by TEM, and microstructural observations of tested samples were correlated with the mechanical response. The SiC/BN fiber coatings effectively inhibited diffusion and reaction at the interface during high-temperature testing. The BN layer also provided a weak interfacial bond that resulted in damage-tolerant fracture behavior. However, oxidation of near-surface SiC fibers occurred during prolonged exposure at high temperatures, and limited oxidation at fiber interfaces was observed when samples were dynamically loaded above the proportional limit stress, creating microcracks along which oxygen could diffuse into the interior of the composite.**

## I. Introduction

FIBER-REINFORCED ceramic-matrix composites are being developed for potential use in gas-turbine engines and other industrial applications involving high service temperatures and both static and dynamic loads. Ceramic materials are often considered for such applications because of their relatively low density and excellent thermal stability, although limited damage tolerance and brittle fracture pose seemingly insurmountable difficulties. However, ceramic composites have shown enhanced fracture toughness and higher damage tolerance compared to monolithic ceramics.[1,2] Critical to the successful implementation of fiber-reinforced ceramic-matrix composites in the aforementioned applications is the presence of a suitably weak fiber/matrix interface that also is resistant to oxidation at high temperatures.[1–5] High strength and toughness at room temperature have been demonstrated in graphite-fiber-reinforced composites and SiC-fiber-reinforced composites with a carbon interfacial layer.[1,2,6,7] However, both of these materials are susceptible to oxidation during long-term high-temperature exposure. Recently, research has been devoted to designing interfaces to improve the oxidation resistance of the composite, and several approaches have been investigated, including the use of fiber coatings and matrix doping.[8–10] For example, nonreacting interfaces have been achieved through fiber coatings, as recently reported in several groups.[11–14] These approaches have achieved partial success, although thermal oxidation, coating uniformity, prohibitive cost, and interface reactions continue to be problematic. Much of the basic research on failure mechanisms in continuous-fiber ceramic composites (CFCCs) has been confined to studies of stress redistribution during loading and evolution of microcracking. Relatively few studies have attempted to combine detailed microscopic observations of interfacial phenomena with mechanical response in high-temperature oxidizing conditions. This approach is particularly promising given the recognized importance of interface phenomena and the fact that the development of ceramic composites is currently driven by potential applications in thermally oxidizing environments. Consequently, one of the primary objectives of the present effort is to determine interface damage mechanisms in a CFCC under thermally oxidizing conditions and to relate these observations to mechanical response.

For the past two decades, fiber-reinforced glass-ceramic composites have been developed and studied at United Technologies Research Center. Recent investigations of a glass-ceramic silicate (barium magnesium aluminosilicate, BMAS) reinforced with continuous-coated SiC fibers have shown that the composite exhibits high flexural strength and toughness, improved flexural creep resistance, and acceptable thermal and environmental stability up to 1200°C compared with similar ceramic composites with glass-ceramic matrices.[15–17]

The objective of the present study was to assess the tensile properties of this composite. Specifically, tensile fracture, tensile creep, and tensile fatigue experiments were conducted in

R. J. Kerans—contributing editor

Manuscript No. 192380. Received August 18, 1995; approved January 9, 1996.
Presented in part at the 1994 TMS Annual Meeting, San Francisco, CA, February 1994 (Control of Interfaces in Metal and Ceramic Composites Symposium).
Supported by the Air Force Office of Scientific Research under Contract No. F49620-92-C-0001 and by the Office of Naval Research (EYS and SRN) under Grant No. N00014-94-1-0728.
*Member, American Ceramic Society.
*Current address: Oak Ridge National Laboratory, Metals and Ceramics Division, Oak Ridge, TN 37831-6068.



15512916, 1996, 6, Downloaded from https://ceramics.onlinelibrary.wiley.com/doi/10.1111/j.1151-2916.1996.tb08760.x by University Of Southern California, Wiley Online Library on [15/11/2022]. See the Terms and Conditions (https://onlinelibrary.wiley.com/terms-and-conditions) on Wiley Online Library for rules of use; OA articles are governed by the applicable Creative Commons License

air at both room temperature and high temperatures. Composite samples were subjected to controlled stress and temperature conditions, and microscopic failure mechanisms were determined. The role of thermal oxidation in the composites also was investigated, and the oxidation behavior under monotonic and cyclic stress conditions was compared.

## II. Materials and Experimental Procedure

### (1) Composite Fabrication

The matrix material selected for the present study was BMAS, formulated to yield stoichiometric barium osumilite ($BaMg_2Al_3(Si_9Al_3O_{30})$) on crystallization. The reinforcement was a Si-C-O fiber (CG-Nicalon, Nippon Carbon Co., Tokyo, Japan) with a dual SiC/BN coating. The coatings were deposited on the fiber by chemical vapor deposition, and the thicknesses of the SiC and the BN layers were ~100 and ~300 nm, respectively. The BN coating had an approximate composition of 40 at.% B, 40 at.% N, 17 at.% C, and <3 at.% O. Carbon was deliberately added to the BN precursor to minimize reactivity during deposition between the BN and the Nicalon fibers. The SiC overcoating was applied to the BN-coated fibers to prevent boron diffusion into the matrix during composite fabrication. The oxygen content of both the SiC and the BN layers was measured by Auger spectroscopy to be <3%.[15] The measured tensile strength of the coated fiber (2220 ± 565 MPa) indicated that essentially no degradation in ultimate strength was caused by the coating process.[3,9]

The composite was fabricated by hot pressing a layup of 0°/90° plies in graphite dies at 1450°C in flowing argon. The pressing time was 5 min, and the pressure was 6.9 MPa. The resulting composite was >98% of theoretical density, and the resulting fiber loading was ~50 vol%. After it was hot pressed, the panel was machined into dogbone tensile samples (25 mm gauge length, 5 mm thick) and heat-treated ("ceramed") in argon at 1200°C for 24 h to crystallize the BMAS matrix to the barium osumilite phase. After the samples were ceramed, the amount of residual intergranular glassy phase in the BMAS matrix was ~3–5 vol%. All of the samples for mechanical testing were machined from a single composite panel to minimize effects of variations in material. Extensive testing on similar composites yielded results similar to those reported here.

### (2) Mechanical Testing

All of the mechanical testing was conducted in air with a relative humidity of 40%–70%, and all samples were oriented such that the 0° plies were aligned with the maximum principal stress ($\sigma_1$). Uniaxial tensile experiments were performed at 20° (room temperature), 1100°, and 1200°C. Specimens were heated to the test temperature in 10–15 min and held without load for 10 min. The load was steadily increased using a crosshead speed of 0.05 cm/min ($\dot{\varepsilon} \approx 3 \times 10^{-4}\ s^{-1}$) or ~5 MPa·s$^{-1}$ until fracture occurred (usually in ~1 min). The specimens were then cooled to ambient temperature in ~5 min. Tensile creep experiments were performed at 1100°C using stress levels of 103 and 138 MPa. (The proportional limit stress at 1100°C was 88 MPa). In these experiments, specimens with a 25 mm gauge section were gripped outside a hot zone that was 40 mm long, and loads were applied instantaneously (2–3 s). The temperature variation was less than ±10°C within the gauge section, and temperature was monitored by thermocouples embedded in contact extensometer rods. Tensile stress rupture experiments were conducted at 1100° and 1200°C at stress levels of 138 and 69 MPa, respectively. The load was applied at ~5 MPa·s$^{-1}$ and held constant for the duration of the experiment.

Tension–tension fatigue testing was conducted at 20°, 1100°, and 1200°C. The loading apparatus consisted of an articulated gripping system, resistance heater ($MoSi_2$), and quartz rod extensometer, all of which were on a closed loop servohydraulic testing system. The gripping system consisted of cold pin-loaded friction grips. All tests were conducted at a stress ratio ($\sigma_{min}/\sigma_{max}$) of 0.1, and $\sigma_{max}$ values of 103 and 138 MPa, equal to the stress levels used in the creep experiments. The samples were subjected to $10^5$ cycles or until failure occurred, whichever came first. The frequency was between 2 and 3 Hz, which resulted in a $10^5$ cycle runout time of 9–13 h. An acoustic emission sensor (70–150 kHz resonant frequency) was mounted on the cold grip, and the signal was sent to a personal analog computer system for data acquisition and analysis. In addition, the cycle count signal was sent from the waveform generator to the PAC system so that acoustic emission activity could be monitored for each cycle.

### (3) Composition and Microstructure Observations

The fracture surfaces of samples tested in monotonic tension and of samples failed during the creep and fatigue experiments were examined using scanning electron microscopy (SEM). Structural analysis of tensile creep samples was conducted using X-ray diffractometry (XRD), and the results were compared with the as-ceramed composites. Some tested samples were ground to powders and analyzed to determine possible changes in matrix phases, while others were analyzed as-tested to determine the phases present in surface scales. Microstructures of the composites were characterized using transmission electron microscopy (TEM). Thin foils were sectioned in different orientations from ~5 mm below the fracture surface in fractured samples. Sections taken closer to the fracture surface were prohibitively fragile, implying a near-surface damage zone. Specimens were prepared in a conventional manner by mechanical polishing, dimpling, and ion milling. Thinned sections were examined using an electron microscope (Model 2010, JEOL, Tokyo, Japan) equipped with a thin-window X-ray spectrometer and a Gatan parallel detection electron energy loss spectrometer (PEELS). The local composition of selected regions of interest in TEM specimens was measured using energy dispersive spectroscopy (EDS) and PEELS. Probe sizes of 10 or 15 nm were used.

## III. Results and Discussion

### (1) Tensile Experiments

*(A) Tensile Properties:* The composite exhibited ultimate tensile strengths (UTS) of 230–300 MPa at all test temperatures. Figure 1 shows tensile stress–strain curves for tests conducted at 20°, 1100°, and 1200°C, and the corresponding property values are listed in Table I. In all cases, the composites exhibited elastic deformation upon initial loading, from which an elastic modulus was determined. (The modulus was estimated over the stress range of 0–50 MPa). The stress at which the curve deviated from linearity marked the proportional limit (PL), defined here using an offset of 0.05%. The deviation from elastic behavior is often attributed to initiation of matrix microcracking, although recent studies have shown that microcracking usually initiates well below the proportional limit.[18–20] Beyond the PL, the stress continued to increase, reaching an UTS in the range of 230–300 MPa, whereupon the composites failed. No degradation in UTS was observed at high temperatures. The UTS and the strain-to-failure ($\varepsilon_f$) of the composites increased with increased temperature, while the elastic modulus decreased. However, the PL was unchanged from 20° to 1100°C, and decreased by about 20% at 1200°C. The observed behavior is discussed in further detail in Section III(*1*)(*C*).

*(B) Fracture Surface:* The fracture surfaces of composite samples tested at 20° and 1100°C were fibrous in nature, indicating extensive fiber pullout and crack deflection along interfaces during fracture (Fig. 2(A)). The length of the pulled-out fibers in the 0° plies was ~50–200 μm, and they appeared slightly longer in the samples tested at high temperature. Further examination of the room-temperature sample by SEM and TEM revealed that debonding occurred primarily in the BN coating layer, and fibers frequently showed regions in which the coating was partly debonded and partly adherent. The experiment at 1100°C lasted for ~20 min (including 15 min heating without load, 1 min under load, and a few minutes to cool

15512916, 1996, 6, Downloaded from https://ceramics.onlinelibrary.wiley.com/doi/10.1111/j.1151-2916.1996.tb08760.x by University Of Southern California, Wiley Online Library on [15/11/2022]. See the Terms and Conditions (https://onlinelibrary.wiley.com/terms-and-conditions) on Wiley Online Library for rules of use; OA articles are governed by the applicable Creative Commons License

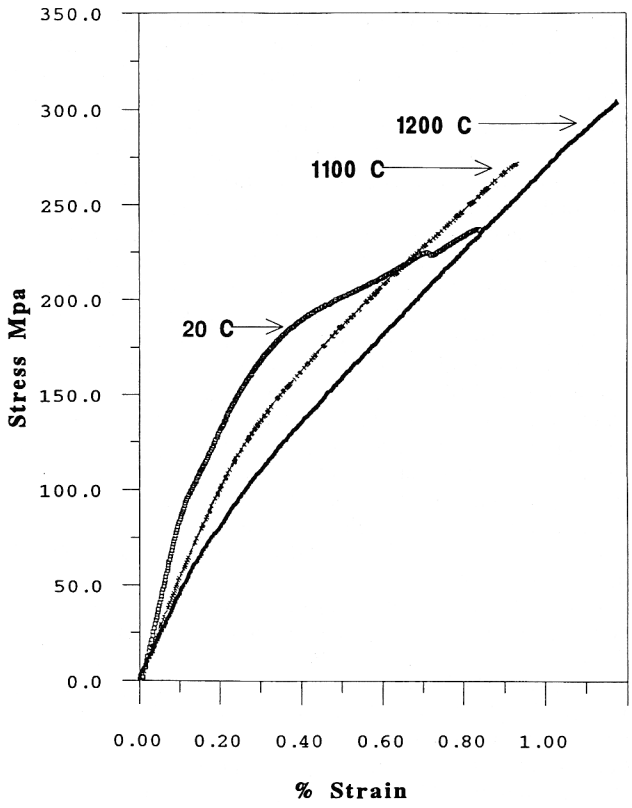


**Fig. 1.** Monotonic tensile stress versus strain response of BMAS/SiC/BN/Nicalon fiber composites tensile tested at 20°, 1100°, and 1200°C ($\dot{\varepsilon} = 3 \times 10^{-4}\ s^{-1}$).

**Table I. Tensile Properties of BMAS/SiC/BN/SiC Fiber Composites***

| Temperature (°C) | PL (MPa) | E (GPa) | UTS (MPa) | $\varepsilon_f$ (%) |
|---|---|---|---|---|
| 20 | 87.9 | 98.3 | 236.5 | 0.84 |
| 1100 | 88.0 | 54.3 | 271.6 | 0.94 |
| 1200 | 70.1 | 44.0 | 302.7 | 1.18 |

*Each data point represents a single test ($\dot{\varepsilon} \approx 3 \times 10^{-4}\ s^{-1}$).

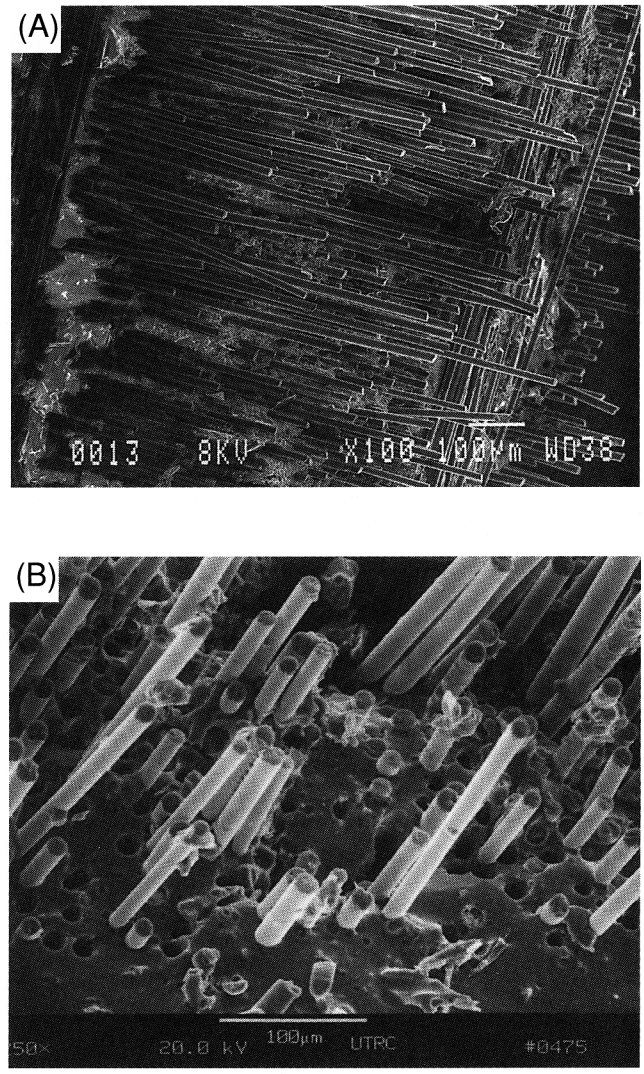


**Fig. 2.** Fracture surface of the composites tested at (A) 1100° and (B) 1200°C.

down), during which time there was no significant change in the microstructure or degradation in strength or toughness. The observations of a fibrous fracture surface and debonding within the BN layer indicated that a weak interfacial bond was achieved by the dual coating, as intended. The weak bond allowed transverse cracks in the matrix to deflect along the fiber/matrix interface, resulting in increased strength and tough fracture behavior.

The fracture surface of the composite tested at 1200°C exhibited different features. A glassy surface layer appeared in matrix regions of the fracture surface, as shown in Fig. 2(B). The newly formed glass was porous, and the pores tended to be clustered around the 0° plies. The porous surface layer was attributed to oxidation of the SiC fibers and the coating layers *after* composite failure, which resulted in formation of siliceous glass and CO gas. Before the fractured composite had time to cool, this glassy phase could also penetrate into cracks and/or delaminations formed as a result of composite fracture.

*(C) Microstructure Observations:* Microstructural analysis of the tensile-tested composites was conducted using TEM. Particular attention was directed to the fiber/matrix interfacial region and the intergranular glass phase in the BMAS matrix. Compared to the ceramed condition, no distinct changes were observed at the matrix/coating interface, the SiC/BN interface, or the BN/fiber interface in any of the tested samples. The SiC fibers, the BN coating, and the SiC coating did not oxidize or react during the experiments, except when exposed to air at the fracture surface and at microcracks. Debonding appeared to occur primarily in the BN coating, an observation consistent with results described in the previous subsection.

Intergranular glassy phase was prevalent in the matrix and had important effects on the tensile properties of the composites. The BMAS matrix crystallized primarily to the barium osumilite phase, but contained ~3–5 vol% residual glassy phase present as thin intergranular films, as shown in Fig. 3. The glass phase in this particular region was thick, and thinner glass films were prevalent along most matrix grain boundaries, indicating wetting. The glass composition was measured by EDS and showed a conspicuous absence of magnesium, but was otherwise similar to the barium osumilite grains. At high temperatures (1100° and 1200°C), these intergranular glass films presumably became less viscous, facilitating boundary sliding, and rendering the matrix more susceptible to damage processes, such as cavitation.[21] These phenomena effectively increased the matrix compliance, contributing to the observed decrease in modulus and proportional limit stress (the loading rates were similar at all temperatures). In contrast, the strength of the Nicalon fibers did not degrade appreciably at this temperature, particularly for the times involved.[22,23] Consequently, the fibers carried most of the load, and the matrix carried relatively little. Thus, the overall effect of matrix softening at high temperature was that the composite became more damage tolerant, resulting in an increase in both UTS and strain-to-failure.

15512916, 1996, 6, Downloaded from https://ceramics.onlinelibrary.wiley.com/doi/10.1111/j.1551-2916.1996.tb08760.x by University Of Southern California, Wiley Online Library on [15/11/2022]. See the Terms and Conditions (https://onlinelibrary.wiley.com/terms-and-conditions) on Wiley Online Library for rules of use; OA articles are governed by the applicable Creative Commons License

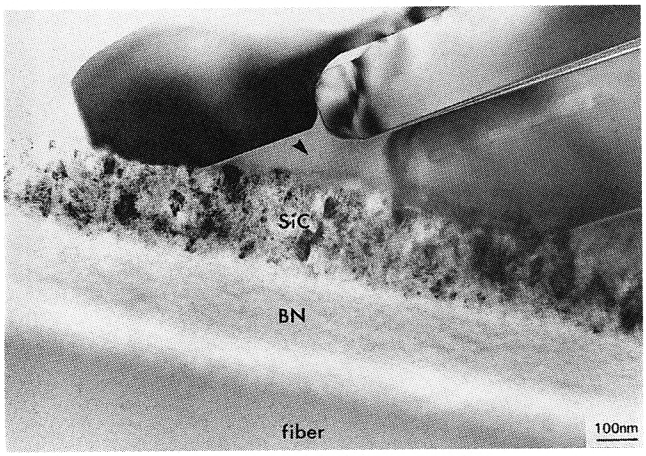


**Fig. 3.** Interfacial region of the composite showing SiC fiber, SiC/BN layers, BMAS grains, and intergranular glassy phase (arrow) (Ref. 12).

### (2) *Tensile Creep*

*(A) Creep Properties:* Tensile creep experiments at 1100°C produced strain versus time curves similar to the one shown in Fig. 4. A transient creep mode in which the strain rate gradually decreased was observed for ~50 h (the data gap shown was caused by an electronic malfunction). The sample then experienced a low and nominally constant creep rate that continued until the experiment was terminated (without failure) at 266 h. The measured creep rate in this regime was $2.3 \times 10^{-9}$ $s^{-1}$. A second sample was crept for 65 h at 138 MPa, and it failed when uploaded to 165 MPa. The creep behavior of this sample was similar to the first sample, and the creep rate after the transient regime also was $\sim 10^{-9}$ $s^{-1}$.

Comparing these results to the creep response reported for similar materials provides additional insight into the observed behavior. For example, flexural creep experiments conducted on identical material in air at 1100°C also resulted in a nominally constant creep rate in the range of $10^{-9}$ $s^{-1}$ after a period of transient creep.[17] The low creep rates in both cases derive from the creep resistance of the fibers under these stress–temperature conditions.[23] Consequently, nearly all of the load is carried by the fibers, which are elastically loaded and constrain the less creep-resistant matrix. This phenomenon is not uncommon in the tensile creep of fiber-reinforced ceramics[24,25] and is reportedly desirable.[26] On the other hand, there is a substantial transient (primary creep) response, which, in fact, accounts for most of the measured strain. The large transient relates to stress redistribution processes occurring in the composite and to the intrinsic response of the glass-ceramic.[24,27] This redistribution of stress may involve one or more of the following processes: redistribution of residual intergranular glass phase; straightening of fibers; and/or compliance of the interface. Meyer *et al.*[27] systematically explored the role of the interface response in the compressive creep behavior of unidirectional glass-ceramic composites. From their experiments, they concluded that plastic flow of an interface layer of siliceous glass emulated a debonded interface and contributed substantially to the observed creep response, although most of the transient strain reportedly derived from redistribution of *intergranular* matrix glass. In the present study, the weak interfacial bond provided by the BN coating may facilitate the redistribution of stress in a similar fashion during primary creep, particularly in the vicinity of stress concentrations such as microcracks, where debonding is observed in TEM replicas.[15] However, the extent to which the turbostratic BN layer is able to actually flow at high temperatures is presently not known, and there are likely to be substantial differences associated with tensile loading compared to compressive loading that promotes shear stress on the fiber/matrix interface.[27] Nonetheless, the tensile creep rate of the composite at stress levels of ~50% of the UTS at 1100°C is barely measurable.

Tensile stress rupture experiments at 1100° and 1200°C lasted longer than one year. The sample tested at 1100° endured 1.7 years at a stress of 138 MPa (well above the fast-fracture PL stress of 88 MPa) before a grip failure occurred, terminating the experiment. The sample was then reloaded in uniaxial tension at 1100°C and stressed to failure. The retained tensile strength was 248 MPa, slightly less than the nominal fast-fracture strength (272 MPa) at this temperature. A similar experiment conducted at 1200°C lasted 1.3 years before failing at a stress 40% greater than the fast-fracture PL stress at 1200°C.

*(B) Microstructural Observations:* Microstructural analysis of the tensile creep samples revealed a variety of changes in the interface microstructure. In the first sample, crept for 266 h at 103 MPa, no gross changes were observed at the fiber/matrix interface in either the 0° or 90° plies, although a subtle interlayer formed at the BN/fiber interface, as shown in Fig. 5(A). Previous studies have shown that this interlayer results from a carbon-condensed oxidation of the SiC fiber.[4,16] The SiC coating, the BN coating, and the SiC fibers showed no other signs of reaction or microstructural change under the conditions used. These observations were consistent with previous studies of the flexural creep behavior of the material at 1100°C, which caused no alteration to the microstructure.[17] However, the interfacial microstructure in the second sample, which was crept for 65 h at 138 MPa, then uploaded to 165 MPa, was quite different from the first sample. As shown in Fig. 5(B), a porous reaction product was formed between the BN coating layer and the SiC fiber in the 90° plies. (The crack

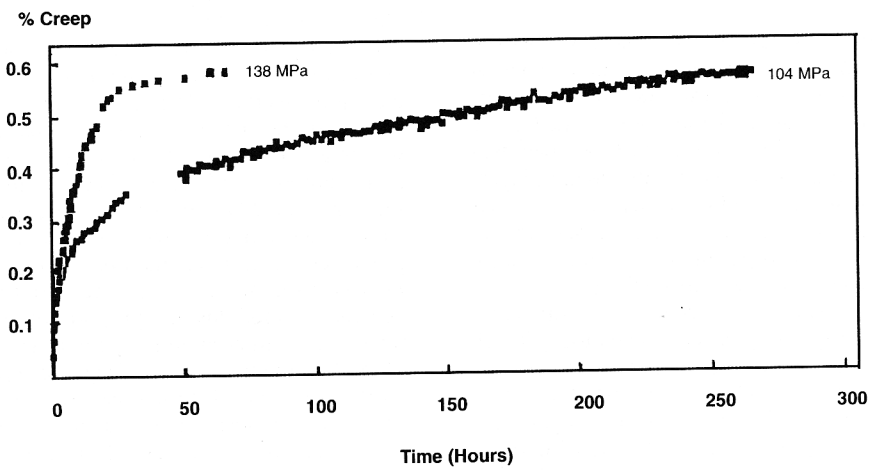


**Fig. 4.** Tensile creep curves for composites tested at 1100°C in air.

15512916, 1996, 6, Downloaded from https://ceramics.onlinelibrary.wiley.com/doi/10.1111/j.1151-2916.1996.tb08760.x by University Of Southern California, Wiley Online Library on [15/11/2022]. See the Terms and Conditions (https://onlinelibrary.wiley.com/terms-and-conditions) on Wiley Online Library for rules of use; OA articles are governed by the applicable Creative Commons License

between the porous reaction product and the SiC fiber was formed during TEM specimen preparation.) Compositional analysis of the reaction product using EDS and PEELS revealed that the porous phase contained only silicon and oxygen, and microdiffraction patterns showed that it was noncrystalline. No compositional changes were detected in the adjoining BN coating or in the fiber interior. A gaseous product apparently evolved during the oxidation reaction, resulting in the observed porosity.

The formation of the glassy reaction product appeared to result from oxidation of fibers exposed to air during creep-crack growth. During the second creep test, the applied stress (138 MPa) was much greater than the PL stress (88 MPa). This presumably caused matrix microcracking and, possibly, interface cavitation,[27] both of which would provide pathways for oxygen access. However, in this experiment, the net creep strains were <1%, and interface cavitation was observed only occasionally. Previous studies with similar composites have shown that cracking caused by tensile loading usually occurs in the BN layer or at the BN/fiber interface.[16] Thus, gaseous diffusion of oxygen along microcracks would be expected to produce the passive oxidation reaction

$$2SiC + 3O_2(g) \rightarrow 2SiO_2 + 2CO(g) \quad (1)$$

Such a reaction would ostensibly result in the observed microstructure if the pores resulted from CO evolution, leaving residual porous $SiO_2$. Note that oxidation of the BN layer (forming borosilicate glass) was not observed in any of the samples, contrary to intuition. Recent thermodynamic analysis has rationalized this phenomenon on the basis of the relative kinetics for oxidation of BN and SiC in systems where the available oxygen is restricted.[28] Oxidation of the SiC fibers was not observed in the composite crept at 103 MPa (without failure), evidently because of the lower density of microcracks and smaller crack openings associated with the lower stress level.

Additional microstructural changes occurred in the BMAS matrix during creep at 1100°C and 103 MPa. The amount of intergranular glassy phase appeared to increase, and, in some cases, the glassy phase was observed to undergo phase separation via spinodal decomposition. (This phenomenon is discussed in detail in Ref. 29.) Furthermore, XRD analysis of crushed composite powders indicated that there was substantially more hexacelsian phase after the creep experiment than before, implying a partial decomposition of the matrix. No decomposition of the matrix was observed in the second sample, in which the creep experiment was of shorter duration.

The fracture surfaces of the tensile stress rupture samples were fibrous in appearance and resembled the tensile fracture surfaces shown in Fig. 2. However, the fracture surfaces also exhibited a peripheral reaction zone in which no pullout was observed. In the sample tested at 1100°C, the width of the reaction zone was ~50 μm, whereas the sample tested at 1200°C showed a reaction zone of ~150 μm. Polished cross sections of the latter sample, shown in Fig. 6, showed reacted fibers and matrix porosity in the peripheral regions, implying an oxidation reaction and the evolution of a gaseous reaction product. Oxidation of the fibers appeared to occur more extensively in the 90° plies than in the 0° plies. The SiC/BN coatings on the fibers in the 0° plies were unreacted at a subsurface depth of ~150 μm, whereas those in the 90° plies were reacted to a depth of ≥250 μm. The fiber interfaces apparently acted as conduits for accelerated transport of oxygen ("pipeline diffusion"), initiating at fiber ends exposed at the surface. This pipeline diffusion along interfaces in the 90° plies was more rapid than "transverse" diffusion in the 0° plies, where oxygen also must diffuse through the silicate matrix. TEM replica analyses of near-surface and interior regions of the 0° plies showed that, although the near-surface fibers and matrix were severely reacted, the bulk composite, including the dual coating, was unaffected by the severe thermomechanical treatment.

Microstructural analysis of the stress-ruptured composite samples by TEM and XRD revealed that the peripheral reaction zone had undergone a transformation to celsian ($BaAl_2Si_2O_8$, BAS). This transformation involved the oxidation of SiC at and near the surface, leading to the formation of $SiO_2$ and the evolution of CO or $CO_2$ gas. The $SiO_2$ apparently reacted with barium osumilite to form celsian, which implies a volatilization of MgO from the surface region. Celsian is a highly refractory crystalline phase with a melting point >1700°C and a thermal expansion coefficient ($2.29 \times 10^{-6}$/°C) similar to that of barium osumilite (~$3.0 \times 10^{-6}$/°C). The celsian surface scale appeared to function as a passive layer, limiting the diffusion of oxygen

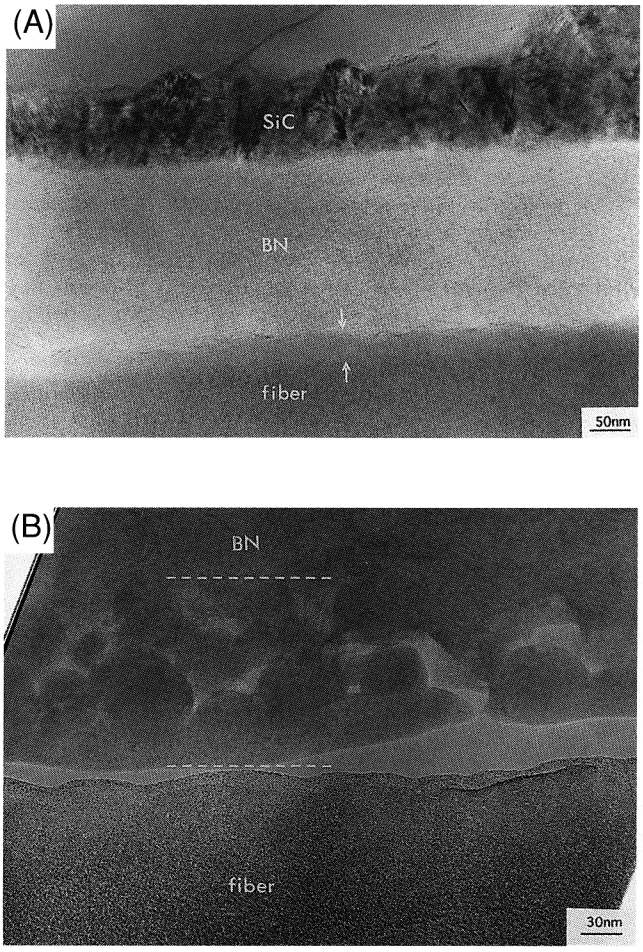


**Fig. 5.** (A) Interfacial region in the composite after tensile creep experiment (1100°C, 103 MPa, air, 266 h) and (B) oxidation occurred at the BN/SiC fiber interface in the composite after tensile creep experiment (1100°C, 138 MPa, air, 65 h).

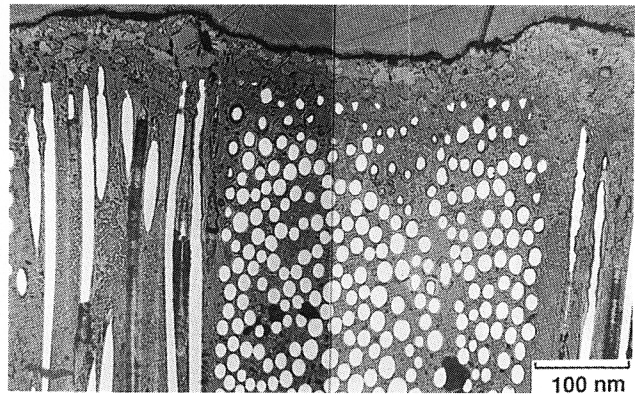


**Fig. 6.** Polished section of composite of tensile stress rupture experiment at 1200°C, 69 MPa, 11 725 h in air.

15512916, 1996, 6, Downloaded from https://ceramics.onlinelibrary.wiley.com/doi/10.1111/j.1551-2916.1996.tb08760.x by University Of Southern California, Wiley Online Library on [15/11/2022]. See the Terms and Conditions (https://onlinelibrary.wiley.com/terms-and-conditions) on Wiley Online Library for rules of use; OA articles are governed by the applicable Creative Commons License

**Table II. Tensile Fatigue Results of BMAS/SiC/BN/SiC Fiber Composites***

| | | | | |
|---|---|---|---|---|
| Temperature (°C) | 20 | 1100 | 1100 | 1200 |
| Maximum stress (MPa) | 103 | 103 | 138 | 103 |
| Comments | $10^5$ cycles, no failure | $10^5$ cycles, no failure | 13 000 cycles, failed | $10^5$ cycles, no failure |

*Air, 2–3 Hz, $\sigma_{min}/\sigma_{max} = 0.1$.

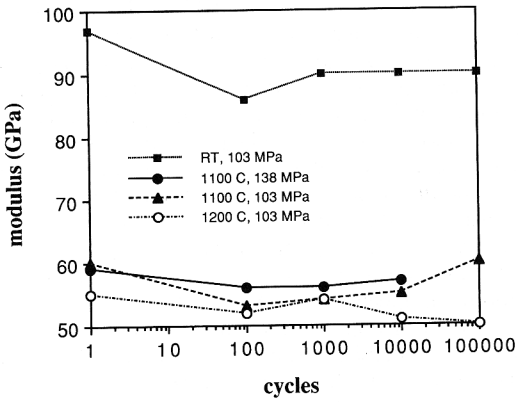


**Fig. 7.** Elastic modulus of the composites determined at different cycle points during the fatigue experiments.

from the test ambient into the bulk, thereby preserving composite properties during long-term mechanical tests.

### *(3) Tensile Fatigue*

*(A) Fatigue Properties:* The results of tensile fatigue experiments are summarized in Table II. When a maximum stress of 103 MPa was used, all of the samples survived $10^5$ cycles without failure. However, at the higher maximum stress (138 MPa), failure occurred at ~13 000 cycles. In addition, changes in the stiffness of the composites during fatigue experiments were monitored by measuring the elastic modulus at the first cycle and after 100, 1000, 10 000, and 100 000 cycles. The results, plotted in Fig. 7, show that the elastic modulus of all the samples decreased 6%–11% from the first to the 100th cycle, and remained relatively constant through the additional cycles. The observed changes in modulus were generally consistent with the acoustic emission data collected during the fatigue experiments, which showed significant activity at cycle one and decreased activity thereafter. Holmes and co-workers[18,30] investigated cyclic fatigue of ceramic composites and found a good correlation between the crack density, measured by replicas, and the initial modulus decrease. In the current work, TEM replicas of tensile fatigue samples showed matrix cracks that extended from fiber to fiber, connected by segments of debonded BN layer.[15] Thus, the initial decrease in modulus shown in Fig. 7 was attributed to an accumulation of microcracking and fiber/matrix debonding. These damage processes apparently saturated after a relatively small number of cycles (~20). Surprisingly, an apparent increase in stiffness of 7 GPa was evident between $10^4$ and $10^5$ cycles in one of the fatigue samples ($T$ = 1100°C and $\sigma_{max}$ = 103 MPa). Recovery of the elastic modulus during cyclic loading has often been reported in other fiber-reinforced glass- or glass-ceramic-matrix composites.[31,32] Although the causes of this phenomenon are not fully understood, Zawada *et al.*[31] and Holmes and co-workers[30,32] have speculated that several mechanisms might be responsible, including an increase in the frictional sliding coefficient caused by generation of wear debris at interfaces, crack closure, and/or realignment of the fibers. Based on the microstructural observations presented here, generation of wear debris would appear most likely, although the data are inconclusive, and the modulus recovery measured is small.

*(B) Microstructural Observations:* Microstructural analysis of the tensile fatigue samples revealed several significant features.

(1) In samples fatigued at $\sigma_{max}$ = 103 MPa and 20°C, matrix cracks appeared in both the 0° and 90° plies. The cracks extended to the fibers and along the fiber/matrix interface, as shown in Fig. 8. Although the sites of crack initiation were uncertain, matrix cracks intersected appeared to deflect along debonded interfaces. In most cases, the cracks propagated within the BN layer (Fig. 8(A)) or at the BN/fiber interface (Fig. 8(B)). The BN layer apparently functioned as a debond

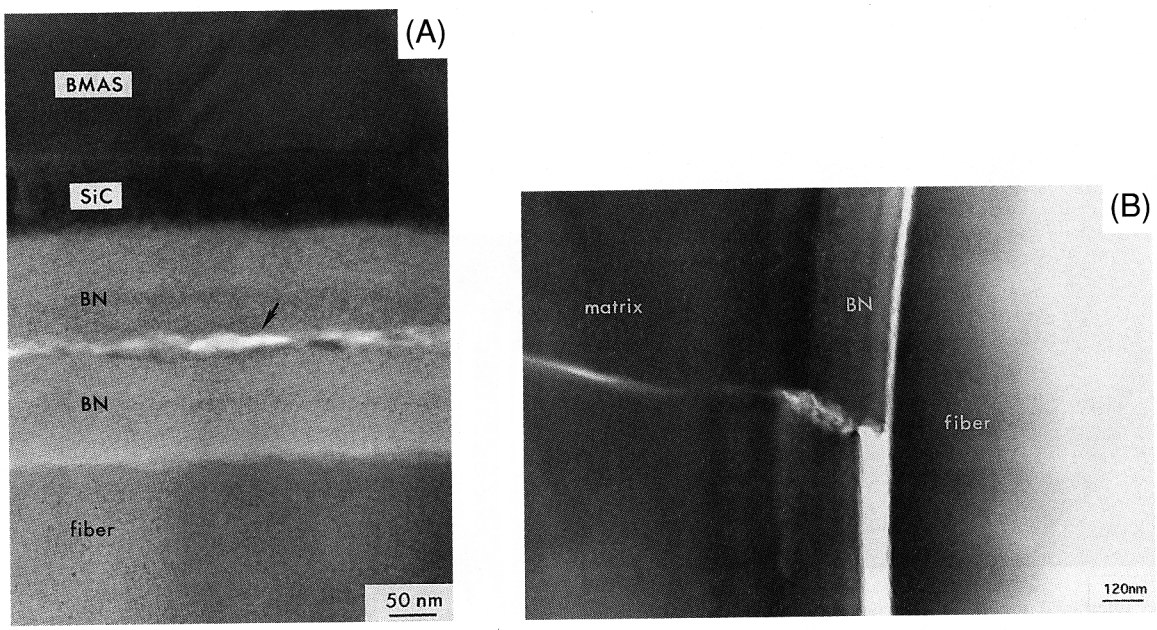


**Fig. 8.** Sample after fatigue testing at 20°C (103 MPa, $10^5$ cycles): (A) crack propagating in the BN layer in the 0° plies and (B) matrix cracks intersecting the BN coating layer in the 90° plies.

15512916, 1996, 6, Downloaded from https://ceramics.onlinelibrary.wiley.com/doi/10.1111/j.1551-2916.1996.tb08760.x by University Of Southern California, Wiley Online Library on [15/11/2022]. See the Terms and Conditions (https://onlinelibrary.wiley.com/terms-and-conditions) on Wiley Online Library for rules of use; OA articles are governed by the applicable Creative Commons License

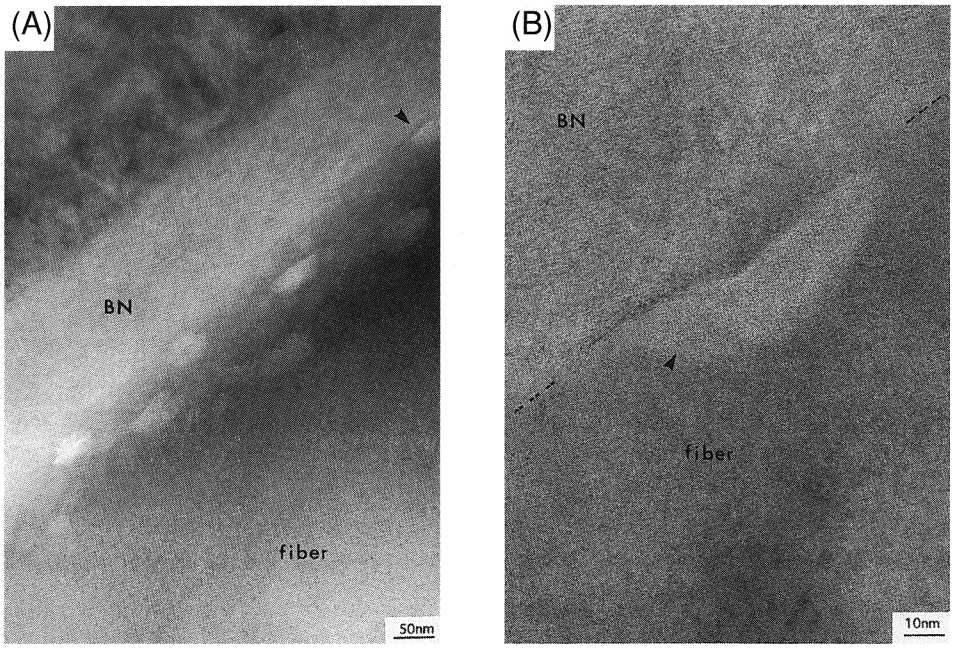


**Fig. 9.** (A) Oxidation of the SiC fiber in an early stage, in the composite fatigued at 1100°C under 103 MPa, and (B) high-resolution image of the arrowed area in (A).

layer, permitting crack deflection and enhancing energy absorption during fracture.

(2) The fatigue samples tested at 1100°C and 103 MPa exhibited fiber oxidation in the 90° plies. Figure 9(A) shows the reaction in an early stage, with affected regions visible as light spots that appear to be on the fiber side of the interface. This is more clearly visible in Fig. 9(B), in which the original fiber surface is highlighted by a dashed line. The affected region is clearly on the fiber side of the interface and appears lighter, whereas the BN coating is largely unaffected. Compositional analysis by EDS and PEELS revealed that such areas contained only silicon and oxygen (no carbon or boron). The absence of carbon was attributed to the oxidation reaction, which resulted in evolution of gaseous CO,[29,33,34] whereas the absence of boron indicated that the BN layer was not involved in the reaction.

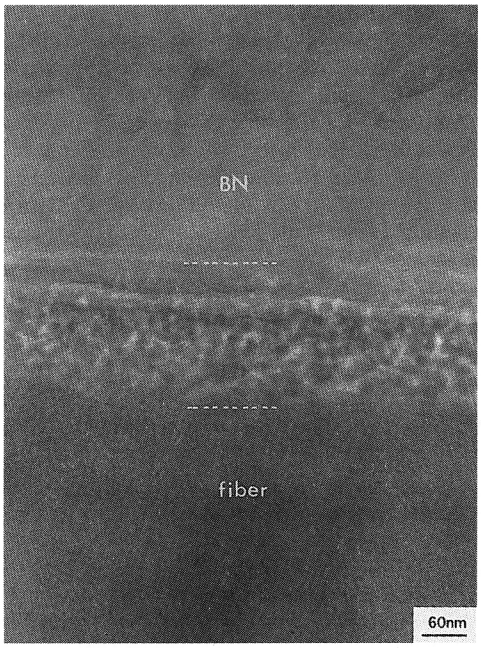


**Fig. 10.** Oxidation of the SiC fiber in an advanced stage.

(The BN layer in Fig. 9(B) does show subtle evidence of what appears to be limited crystallization, i.e., a slightly darker line with lattice fringes between the BN layer and the reacted zone. However, this may instead be evidence of graphitic carbon formed during the initial stages of SiC oxidation,[35] and it is not possible to distinguish between turbostratic BN and carbon because of the thinness of the layer and the structural similarities). When the oxidation reached an advanced stage, a noncrystalline porous layer formed at the BN/fiber interface, exhibiting a characteristic mottled appearance shown in Fig. 10. The thickness of the reacted zone was ~150 μm.

(3) Additional changes were observed in the interior of the SiC fibers in fatigue samples tested at 1200°C. Figures 11(A) and (B) are PEELS spectra collected from the fibers in the ceramed sample and in the fatigued sample, respectively, with selected area diffraction patterns. Both EDS and PEELS measurements indicated that the oxygen concentration increased relative to the pretested fibers. The diffraction pattern from the domains in the fatigued fibers revealed an additional set of reflections. The inner diffuse ring, which was not present in pretested fibers, corresponds approximately to a lattice spacing shared by a group of $SiO_2$ polymorphs (0.342 nm). These observations indicated that the SiC fibers were partly oxidized during fatigue testing, and the oxygen concentration was substantially increased. In contrast, subsurface SiC fibers (>50 μm) showed no signs of oxidation when composites were heat-treated in air at the same temperature (1200°C for 500 h).[16]

The observations described above indicate that oxidation of the SiC fibers was more extensive under cyclic loads than under static loads, even for similar stress levels, times, and temperatures. There are two possible explanations for this phenomenon, neither of which is mutually exclusive. First, the time duration of oxygen exposure may be quite different for the case of the dynamic loading (fatigue) versus static loading (creep). The dynamic loading may very well cause more extensive microcracking in the matrix than static loading, which leads to greater oxygen exposure for the fibers. Second, crack closure in CFCCs can reportedly occur by the oxidation of SiC to produce siliceous glass, as observed in SiC/C/SiC composites.[33] The process of crack closure may be more viable under static applied loads. Recall that, after creep at 1100°C, no oxidation of the SiC fibers was observed (in the bulk) when the applied stress was moderate (103 MPa). Although the applied stress

15512916, 1996, 6, Downloaded from https://ceramics.onlinelibrary.wiley.com/doi/10.1111/j.1551-2916.1996.tb08760.x by University Of Southern California, Wiley Online Library on [15/11/2022]. See the Terms and Conditions (https://onlinelibrary.wiley.com/terms-and-conditions) on Wiley Online Library for rules of use; OA articles are governed by the applicable Creative Commons License

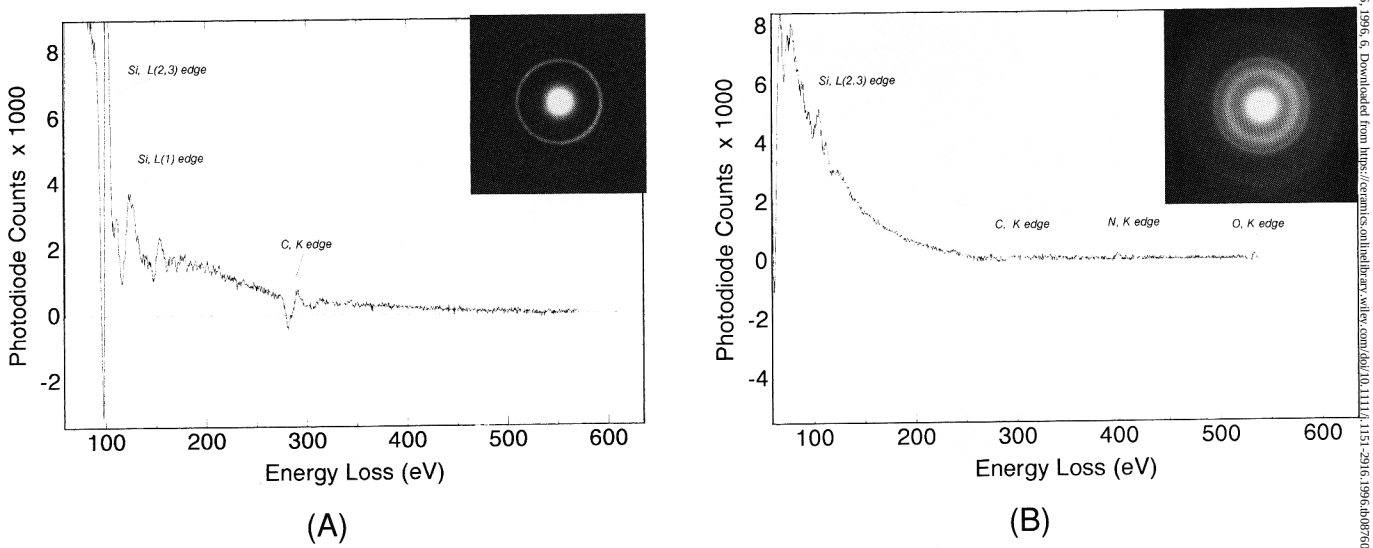


**Fig. 11.** PEELS spectra and diffraction patterns from (A) fibers in the pretested composite and (B) fibers in the fatigued sample (tested in air at 1200°C).

exceeded the PL stress, and, consequently, matrix cracking may well have occurred under these conditions, the crack openings were presumably small enough to be sealed by reaction products. Consequently, oxidation was generally confined to near-surface regions of the composite when the stress level was moderate. Furthermore, thermal exposure alone caused negligible microstructural changes, as in the case of heat treatment in air at the same temperature (1200°C) for 500 h.[16] However, when the (static) applied stress was instantaneously increased to 138 MPa, matrix cracks (or crack-opening displacements) were more extensive, and the crack openings were presumably too large to be sealed by the oxidation product. In this case, oxygen diffused along cracks into the bulk, resulting in oxidation of SiC fibers (Section III(2)(*B*)).

In contrast, under cyclic tensile loads, crack-wake contact prevented accumulation of the oxidation product, thus precluding the possibility of crack healing through the generation of reaction products. Thus, when microcracking occurred, crack healing was prevented, leading to fiber oxidation. Consequently, even with a maximum applied stress of only 103 MPa and comparable loading rates, oxidation of SiC fibers was observed in the bulk composite. This was especially true in the case of fatigue loading at 1200°C, which caused pronounced oxidation of the SiC fibers at the interface. An additional manifestation of the high-temperature oxidation that occurred during cyclic loading was that the fracture surfaces were characterized by fine debris and fragments of debonded coating.[36]

## IV. Conclusions

The tensile properties and corresponding microstructural changes reported here have shown that the fiber coatings effectively inhibited deleterious interface reactions under most of the stress–temperature conditions used. No significant degradation in tensile strength or change in fracture mode was observed up to 1200°C, and the composite exhibited negligible tensile creep rates up to 1100°C. Under cyclic loading to a maximum stress of 103 MPa, the material survived $10^5$ cycles at temperatures up to 1200°C. The short- and long-term properties observed in this study derived largely from the degree to which the interface microstructure was controlled by the SiC/BN dual coating. In particular, the BN coating provided the desired weak interface necessary for high loading-rate toughness, whereas the SiC overlayer provided a barrier to diffusion and reaction at high temperatures. Both layers were more stable in oxidizing atmospheres than either BN coatings alone, or previously studied carbon-rich interfaces.[3,4]

Although the focus of this investigation has undoubtedly been on the interface, the roles of the matrix microstructure and associated properties also are critical. Residual glassy phase in the matrix has important implications on the high-temperature response of the composite. Above 1000°C, viscous flow of intergranular glassy phase facilitated boundary sliding and contributed to matrix softening, allowing the matrix to creep and the fibers to carry most of the applied load. On the other hand, glassy phase in some instances contributed to damage tolerance, allowing microcracks to heal. The matrix properties also controlled the proportional limit stress, the stress at which microcracking was prevalent. Microcracking affected elastic modulus and oxidation resistance, as observed in the creep and fatigue experiments. Microstructural modifications to increase the matrix proportional limit stress should directly benefit the composite properties. Thus, a potentially important area for future research is the design of matrix compositions and microstructures with improved resistance to microcracking. Undoubtedly, there will be tradeoffs in designing composites based on glass-ceramics, in that optimizing stiffness and toughness of the composite by controlling the amount of residual glassy phase also may reduce damage tolerance.

The work presented here also has shown that the microstructures that develop under cyclic stress fields can be quite different from those that evolve under monotonic loading, despite similar stresses and temperatures. In fact, environmental effects had a more significant effect on the material during cyclic loading compared to static or quasi-static loading conditions. Oxidation was enhanced during fatigue experiments, apparently because of crack-wake contact that impeded gaseous diffusion of oxygen. Consequently, material life-time predictions based on experimental data from static loading conditions or in anaerobic environments are likely to be inaccurate when applied to aerobic environments. A more complete understanding of the micromechanisms involved in fatigue damage and the effects of oxidation is needed before introducing the material into high-temperature structural applications.

**Acknowledgments:** The authors are grateful to Jim O'Kelly of 3M for coating the Nicalon fibers used in the study, Stan Kustra of UTRC and Gary Linsey of Pratt & Whitney for mechanical testing of the composites, Anne Staples of Brown University for TEM specimen preparation, and Alexander Pechenik of AFOSR for sponsorship of this program.

## References

[1]K. M. Prewo and J. J. Brennan, "High-Strength Silicon Carbide Fiber-Reinforced Glass-Matrix Composites," *J. Mater. Sci.*, **15**, 463–68 (1980).

[2]K. M. Prewo and J. J. Brennan, "Silicon Carbide-Fiber-Reinforced Glass-Ceramic-Matrix Composites Exhibiting High Strength and Toughness," *J. Mater. Sci.*, **17**, 2371–83 (1982).

15512916, 1996, 6, Downloaded from https://ceramics.onlinelibrary.wiley.com/doi/10.1111/j.1151-2916.1996.tb08760.x by University Of Southern California, Wiley Online Library on [15/11/2022]. See the Terms and Conditions (https://onlinelibrary.wiley.com/terms-and-conditions) on Wiley Online Library for rules of use; OA articles are governed by the applicable Creative Commons License

[3]J. J. Brennan, "Interfacial Characterization of Glass and Glass-Ceramic Matrix/Nicalon SiC Fiber Composites"; pp. 549–60 in *Materials Science Research*, Vol. 20. Plenum Press, New York, 1986.

[4]R. F. Cooper and K. Chyung, "Structure and Chemistry of Fiber–Matrix Interfaces in SiC-Fibre-Reinforced Glass-Ceramic Composites: An Electron Microscopy Study," *J. Mater. Sci.*, **22**, 3148–60 (1987).

[5]R. L. Kerans, R. S. Hay, N. J. Pagano, and T. A. Parthasarathy, "The Role of the Fiber–Matrix Interface in Ceramic Composites," *Am. Ceram. Soc. Bull.*, **68**, 429–42 (1989).

[6]D. C. Phillips, R. A. Sambell, and D. H. Bowen, "The Mechanical Properties of Carbon-Fiber-Reinforced Pyrex Glass," *J. Mater. Sci.*, **7**, 1454–64 (1972).

[7]S. R. Levitt, "High-Strength Graphite Fiber/Lithium Aluminosilicate Composites," *J. Mater. Sci.*, **8**, 793–806 (1973).

[8]R. W. Rice, "BN Coating of Ceramic Fibers for Ceramic Fiber Composites," U.S. Pat. No. 4 642 271, Feb. 10, 1987.

[9]J. J. Brennan, "Interfacial Studies of SiC-Fiber-Reinforced Glass-Ceramic-Matrix Composites," Final Rept. R87-917546-4 on ONR Contract N00014-82-C-0096, Oct. 15, 1987.

[10]R. Naslain, O. Dugne, A. Guette, J. Sevely, C. R. Brosse, J.-P. Rocher, and J. Cotterel, "Boron Nitride Interphase in Ceramic-Matrix Composites," *J. Am. Ceram. Soc.*, **74** [10] 2482–88 (1991).

[11]P. E. D. Morgan and D. B. Marshall, "Functional Interfaces for Oxide/Oxide Composites," *Mater. Sci. Eng.*, **A162** [1–2] 15–26 (1993).

[12]K. Chyung and S. B. Dawes, "Fluoromica-Coated Nicalon-Fiber-Reinforced Glass-Ceramic Composites," *Mater. Sci. Eng.*, **A162** [1–2] 27–34 (1993).

[13]J. Davis and A. G. Evans, "Fiber Coatings for Sapphire-Reinforced Alumina Composites"; pp. 329–36 in *Proceedings of High-Temperature CMCs*, 6th European Conference on Composites Materials (Bordeaux, France, Sept. 20–24, 1993). Woodhead Publishing, Abington Cambridge, England, 1993.

[14]R. F. Cooper and P. C. Hall, "Reactions between Synthetic Mica and Simple Oxide Compounds with Application to Oxidation-Resistant Ceramic Composites," *J. Am. Ceram. Soc.*, **76** [5] 1265–73 (1993).

[15]J. J. Brennan, B. Allen, S. R. Nutt, and Y. Sun, "Interfacial Studies of Coated Fiber-Reinforced Glass-Ceramic-Matrix Composites," Annual Rept. R92-970150-1 on AFOSR Contract F49620-92-C-0002, Nov. 30, 1992.

[16]E. Y. Sun, S. R. Nutt, and J. J. Brennan, "Interfacial Microstructure and Chemistry of SiC/BN Dual-Coated Nicalon-Fiber-Reinforced Glass-Ceramic Composites," *J. Am. Ceram. Soc.*, **77** [5] 1329–39 (1994).

[17]E. Y. Sun, S. R. Nutt, and J. J. Brennan, "Flexural Creep of SiC/BN Dual-Coated-Nicalon-Fiber-Reinforced Glass-Ceramic Matrix Composites," *J. Am. Ceram. Soc.*, **78** [5] 1233–39 (1995).

[18]J. W. Holmes and B. F. Sorensen, "Fatigue Behavior of Continuous-Fiber-Reinforced Ceramic-Matrix Composites"; in *Elevated Temperature Mechanical Behavior of Ceramic Matrix Composites*. Butterworth-Heinemann, Boston, MA, 1995.

[19]P. G. Karandikar and T. W. Chou, "Damage Development and Moduli Reductions in Nicalon–CAS Composites under Static Fatigue and Cyclic Fatigue," *J. Am. Ceram. Soc.*, **73**, 1720–28 (1993).

[20]R. Y. Kim and N. J. Pagano, "Crack Initiation in Unidirectional Brittle-Matrix Composites," *J. Am. Ceram. Soc.*, **74** [5] 1082–90 (1991).

[21]U. Ramamurtry, T. Hansson, and S. Suresh, "High-Temperature Crack Growth in Monolithic and $SiC_w$-Reinforced Silicon Nitride under Static and Cyclic Loads," *J. Am. Ceram. Soc.*, **77** [11] 2985–99 (1994).

[22]B. A. Bender, J. S. Wallace, and D. J. Schrodt, "Effect of Thermochemical Treatments on the Strength and Microstructure of SiC Fibers," *J. Mater. Sci.*, **26**, 970–76 (1991).

[23]G. Simon and A. R. Bunsell, "Creep Behaviour and Structural Characterization at High Temperatures of Nicalon SiC Fibers," *J. Mater. Sci.*, **19**, 3658–70 (1984).

[24]X. Wu and J. W. Holmes, "Tensile Creep and Creep-Strain Recovery Behavior of Silicon Carbide Fiber/Calcium Aluminosilicate Matrix Ceramic Composites," *J. Am. Ceram. Soc.*, **76** [10] 2695–700 (1993).

[25]D. Kervadec and J.-L. Chermant, "Some Aspects of the Morphology and Creep Behavior of a Unidirectional $SiC_f$-MLAS Material"; pp. 459–71 in *Fracture Mechanics of Ceramics*, Vol. 10. Edited by R. C. Bradt, D. P. H. Hasselman, D. Munz, M. Sakai, and V. Ya. Shevchenko. Plenum Press, New York, 1992.

[26]J. W. Holmes and X. Wu, "Elevated Temperature Creep Behavior of Continuous-Fiber-Reinforced Ceramics"; see Ref. 18, pp. 193–260.

[27]D. W. Meyer, R. F. Cooper, and M. E. Plesha, "High-Temperature Creep and the Interfacial Response of a Ceramic-Matrix Composite," *Acta Metall. Mater.*, **41** [11] 3157–70 (1993).

[28]B. W. Sheldon, E. Y. Sun, S. R. Nutt, and J. J. Brennan, "Oxidation of BN-Coated SiC Fibers in Ceramic Matrix Composites," *J. Am. Ceram. Soc.*, **79** [2] 539–43 (1996).

[29]E. Y. Sun, "Fiber-Reinforced Glass-Ceramic Matrix Composites for High-Temperature Applications"; Ph.D. thesis. Brown University, Providence, RI, 1994.

[30]J. W. Holmes and C. Cho, "Experimental Observations of Frictional Heating in a Fiber-Reinforced Ceramic," *J. Am. Ceram. Soc.*, **75** [4] 929–38 (1992).

[31]L. P. Zawada and L. M. Butkus, "Tensile and Fatigue Behavior of Silicon Carbide-Fiber-Reinforced Aluminosilicate Glass," *J. Am. Ceram. Soc.*, **74** [11] 2851–58 (1991).

[32]S. F. Shuler, J. W. Holmes, X. Wu, and D. Roach, "Influence of Loading Frequency on the Room-Temperature Fatigue of a Carbon-Fiber/SiC-Matrix Composite," *J. Am. Ceram. Soc.*, **76** [9] 2327–36 (1993).

[33]L. Filipuzzi, G. Camus, and R. Naslain, "Oxidation Mechanisms and Kinetics of 1D-SiC/C/SiC Composite Materials: I, An Experimental Approach," *J. Am. Ceram. Soc.*, **77** [2] 459–66 (1994).

[34]Y. Ramakrishnan and N. Jayaraman, "Fatigue Behavior of Borosilicate Glass-Ceramic Matrix Nicalon (Silicon Carbide) Fiber Composites," *J. Mater. Sci.*, **28**, 5580–91 (1993).

[35]F. Lin, T. N. Marieb, A. A. Morrone, and S. R. Nutt, "Thermal Oxidation of $Al_2O_3$–SiC Whisker Composites: Mechanisms and Kinetics," *Mater. Res. Soc. Symp. Proc.*, **120**, 323–32 (1988).

[36]J. J. Brennan, S. R. Nutt, and Y. Sun, "Interfacial Studies of Coated-Fiber-Reinforced Glass-Ceramic-Matrix Composites," Annual Rept. R93-970150-2 on AFOSR Contract F49620-92-C-0001, Nov. 30, 1993. □

15512916, 1996, 6, Downloaded from https://ceramics.onlinelibrary.wiley.com/doi/10.1111/j.1151-2916.1996.tb08760.x by University Of Southern California, Wiley Online Library on [15/11/2022]. See the Terms and Conditions (https://onlinelibrary.wiley.com/terms-and-conditions) on Wiley Online Library for rules of use; OA articles are governed by the applicable Creative Commons License